BIOCHEMISTRY
including biophysical chemistry & molecular biology

Article

pubs.acs.org/biochemistry

Botulinum Neurotoxin G Binds Synaptotagmin-II in a Mode Similar to That of Serotype B: Tyrosine 1186 and Lysine 1191 Cause Its Lower Affinity

Gesche Willjes,[†] Stefan Mahrhold,[†] Jasmin Strotmeier,[‡] Timo Eichner,[§] Andreas Rummel,[‡] and Thomas Binz*[,†]

[†]Institut für Physiologische Chemie, OE 4310, und [‡]Institut für Toxikologie, OE 5340, Medizinische Hochschule Hannover, Carl-Neuberg-Straße 1, 30625 Hannover, Germany

[§]Department of Biochemistry, Brandeis University, Waltham, Massachusetts 02454, United States

ABSTRACT: Botulinum neurotoxins (BoNTs) block neurotransmitter release by proteolyzing SNARE proteins in peripheral nerve terminals. Entry into neurons occurs subsequent to interaction with gangliosides and a synaptic vesicle protein. Isoforms I and II of synaptotagmin were shown to act as protein receptors for two of the seven BoNT serotypes, BoNT/B and BoNT/G, and for mosaic-type BoNT/DC. BoNT/B and BoNT/G exhibit a homologous binding site for synaptotagmin whose interacting part adopts helical structure upon binding to BoNT/B. Whereas the BoNT/B−synaptotagmin-II interaction has been elucidated in molecular detail, corresponding information about BoNT/G is lacking. Here we systematically mutated the synaptotagmin binding site in BoNT/G and performed a comparative binding analysis with mutants of the cell binding subunit of BoNT/B. The results suggest that synaptotagmin takes the same overall orientation in BoNT/B and BoNT/G governed by the strictly conserved central parts of the toxins' binding site. The surrounding nonconserved areas differently contribute to receptor binding. Reciprocal mutations Y1186W and L1191Y increased the level of binding of BoNT/G approximately to the level of BoNT/B affinity, suggesting a similar synaptotagmin-bound state. The effects of the mutations were confirmed by studying the activity of correspondingly mutated full-length BoNTs. On the basis of these data, molecular modeling experiments were employed to reveal an atomistic model of BoNT/G−synaptotagmin recognition. These data suggest a reduced length and/or a bend in the C-terminal part of the synaptotagmin helix that forms upon contact with BoNT/G as compared with BoNT/B and are in agreement with the data of the mutational analyses.

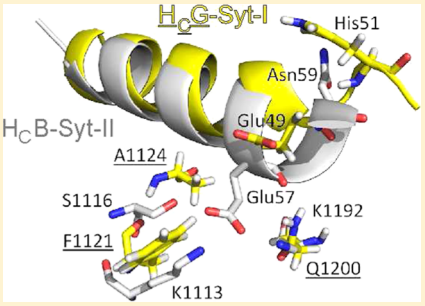

The disease botulism is characterized by flaccid paralysis that may lead to respiratory failure and death and can affect humans and a variety of animal species. It is caused by botulinum neurotoxin (BoNT), which exists in seven serologically different types that are produced by various bacteria of the genus *Clostridium* (BoNT/A−G). In addition, mosaic-type BoNTs that comprise sections of two different serotypes have been described.[1] They all exhibit a highly related tertiary structure consisting of a disulfide bond-connected light chain and heavy chain.[2] The latter is responsible for specific binding to motoneurons, receptor-mediated endocytosis, and translocation of the light chain from the endosomal compartment into the cytosol.[3] The light chains of BoNT/B, -D, -F, and -G proteolyze VAMP (vesicle-associated membrane protein)/synaptobrevin-2 and those of BoNT/A, -C, and -E SNAP-25 (synaptosomal-associated protein of 25 kDa). The light chain of BoNT/C cleaves in addition HPC1/syntaxin 1. The three substrates together form the core of the neuronal SNARE complex.[4] SNARE cleavage abrogates the fusion of synaptic vesicles with the presynaptic membrane and thus the release of acetylcholine.

It has long been known that complex glycosphingolipids, gangliosides, that are highly enriched in neuronal tissue act as receptors for BoNTs.[5] Whereas there is evidence that gangliosides are the sole receptors for BoNT/C,[6,7] the entry of the remaining BoNTs has been shown to depend upon the additional interaction with the intravesicular domain of a synaptic vesicle protein that becomes transiently exposed on the cell surface in the course of the synaptic vesicle cycle. In this scenario, gangliosides are assumed to concentrate BoNTs on the presynaptic membrane and thereby to increase the likelihood that the toxins encounter their protein receptor.[8] BoNT/A, BoNT/E,[9−11] and probably also BoNT/D and BoNT/F[12,13] utilize the synaptic vesicle glycoprotein 2 (SV2) as a protein receptor. BoNT/B, BoNT/G, and mosaic-type BoNT/DC have been demonstrated to harness isoforms 1 and 2 of synaptotagmin (Syt) as receptors.[14−18]

BoNT/A, -B, -E, -F, and -G exhibit a highly conserved ganglioside binding pocket located in homologous positions within the C-terminal domain of the cell-binding subunit (H_C fragment). This binding pocket is characterized by the primary structure motif Glu...His...SerXxxTrpTyr...Gly, in which Glu is

Received: March 19, 2013
Revised: May 6, 2013
Published: May 6, 2013

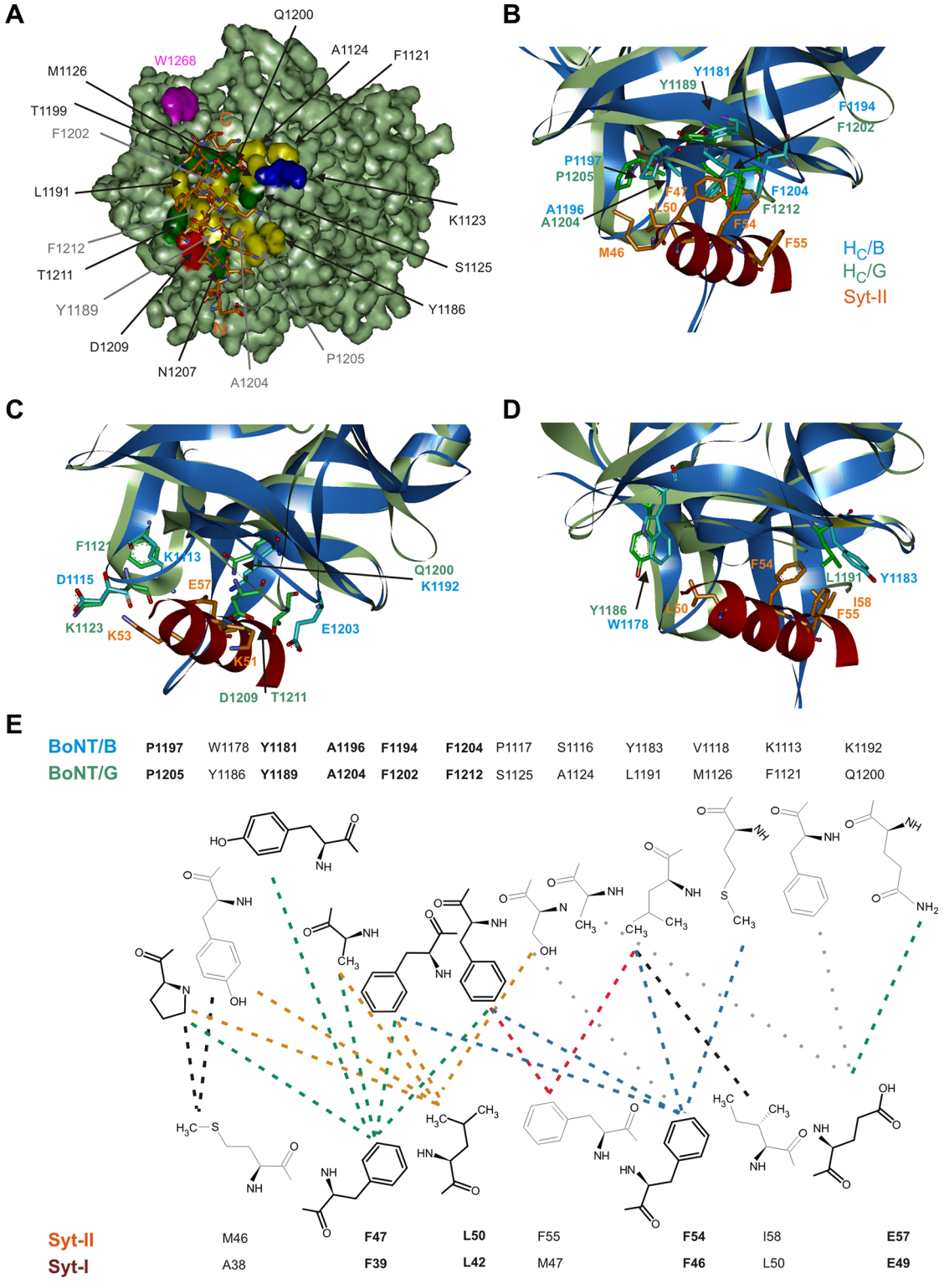

Figure 1. Structural analysis of the likely BoNT/G−Syt-II interaction. (A−D) Superposition of the Syt-II-bound structure of H_CB (PDB entry 2NM1) with that of H_CG (PDB entry 2VXR). (A) H_CG is depicted as a surface plot and Syt-II as a stick model, whereas H_CB is omitted. Residues of H_CG that are supposed to interact with Syt-II are colored and specified. As a point of reference, the central residue of the ganglioside binding pocket, W1268, is also shown (magenta). (B−D) Secondary structure plot of H_CB (blue), H_CG (pastel green), and Syt-II (orange-brown). Interacting amino acids are shown as sticks. Panel B illustrates H_CB and H_CG residues forming the central part of the Syt-II binding site. Panel C illustrates residues located around the central part of the binding site, whereas panel D depicts amino acids whose reciprocal exchange increased the binding affinity of H_CG. (E) Schematic representation of the probable H_CG−Syt-II interface. The equivalent residues of H_CB and Syt-I are also shown. Conserved residues are shown in bold. Proposed H_CB−Syt-II interactions that cannot form between H_CG and Syt-II are indicated by dotted lines, whereas maintained interactions are shown as colored dashed lines.

dx.doi.org/10.1021/bi4003502 | *Biochemistry* 2013, 52, 3930−3938

substituted with glutamine in BoNT/G and His is replaced with lysine and glycine in BoNT/E and BoNT/G, respectively.[5] Available data for BoNT/A, BoNT/B, and BoNT/F show that this pocket preferentially binds trisialoganglioside GT1b followed by disialoganglioside GD1a. Other gangliosides bind far less efficiently.[19−21] A cocrystal structure of BoNT/A-H_C (H_CA) bound to GT1b-β revealed that the terminal *N*-acetylgalactosamine-3-galactose-4-sialic acid-5 of GT1b (being also present in GD1a, but absent, e.g., in GD1b) is positioned in the binding pocket cavity.[22] The ganglioside preferences of BoNT/E and BoNT/G have been poorly studied.

The protein receptor binding site has only been localized for those BoNTs that utilize synaptotagmin. This binding site is located adjacent to but does not overlap with the ganglioside binding pocket in BoNT/B and BoNT/G at the C-terminal tip of the H_C fragment.[23] Structural data of a cocrystal of the luminal domain of Syt-II bound to BoNT/B identified a saddle-shaped crevice that mediates the interaction with Syt-II.[24,25] Binding is in particular mediated by hydrophobic interactions but also by one major salt bridge (Figure 1E). As shown by *in vitro* binding experiments, the affinity of BoNT/B and BoNT/G for the luminal domain of Syt-I and Syt-II decreases in the order B-Syt-II ≫ G-Syt-I > G-Syt-II ≫ B-Syt-I,[23] although the hydrophobic character of the crucial toxin residues responsible for the hydrophobic interactions is well conserved between BoNT/B and BoNT/G (Figure 1B,E). The far higher affinity for Syt-II is one aspect that explains the higher *in vivo* toxicity of BoNT/B.[14,15]

Here we characterize the interaction of BoNT/G, which occasionally causes botulism,[26] with its cellular receptors. We show that BoNT/G like BoNT/B preferentially binds gangliosides GT1b and GD1a. Binding and neurotoxicity assays of systematically mutated BoNTs and Syt-II, including reciprocal mutations between BoNT/B and BoNT/G, combined with molecular modeling studies furthermore show that synaptotagmin adopts helical structure upon contact with BoNT/G, which is probably shorter and/or bent as compared with the structure induced upon contact with BoNT/B. In addition, a tryptophan to tyrosine mutation and a tyrosine to leucine mutation in BoNT/G were identified as the main determinants for the lower affinity of BoNT/G versus BoNT/B for the protein receptor Syt.

EXPERIMENTAL PROCEDURES

Protein Structure Analyses. Structure analyses, structure superposition, and creation of images were conducted using Discovery Studio Visualizer version 2.5 (Accelrys, Cambridge, U.K.) employing PDB entries 2VXR (BoNT/G-H_C[27]) and 2NM1 (BoNT/B-H_C−Syt-II[25]).

Plasmid Constructions. Plasmids encoding the H_C fragment (pH_CBS and pH_CGS) and full-length BoNT (pBoNTBS and pBoNTGS-Thro) of serotypes B (strain B1, okra) and G as well as the plasmids encoding GST fusion proteins of rat Syt-I(1−53) and rat Syt-II(1−61) have been described previously.[18,28] The H_C fragment and Syt-II mutants were generated by polymerase chain reaction by applying the GeneTailor site-directed mutagenesis system (Life Technologies, Darmstadt, Germany) and suitable primers. Mutated expression plasmids for full-length BoNT/B and BoNT/G were generated by swapping mutated DNA fragments of pH_CBS or pH_CGS in the pBoNTBS or pBoNTGS-Thro plasmid, respectively, using suitable endonuclease restriction sites. For ganglioside binding assays, a BoNT/G-H_C (H_CG) variant carrying an N-terminal His tag followed by a triple FLAG tag, including an enterokinase recognition site (amino acid sequence, MRGSHHHHHHGS DYKDHDG DYKDHDI DYKDDDDKGS), was generated. Nucleotide sequences of all mutants were verified by DNA sequencing.

Purification of Recombinant Proteins. Wild-type and mutated recombinant H_C fragments and full-length BoNTs were produced, the latter under biosafety level 2 containment (Project GAA A/Z 40654/3/57), utilizing *Escherichia coli* strain M15pREP4 (Qiagen) during a 16 h induction at 21 °C in the presence of 0.25 mM IPTG and purified on StrepTactin-Sepharose beads (IBA GmbH) according to the manufacturer's instructions. Fractions containing the desired proteins were pooled, H_C fragments were additionally dialyzed against 20 mM Tris-HCl and 150 mM NaCl (pH 7.2), frozen in liquid nitrogen, and kept at −70 °C. Protein concentrations and the extent of hydrolytic activation of full-length BoNT caused by *E. coli* proteases during purification were determined subsequent to sodium dodecyl sulfate−polyacrylamide gel electrophoresis (SDS−PAGE) and Coomassie Blue staining by using a LAS-3000 imaging system (Fuji Photo Film, Co., Ltd.), AIDA version 2.11, and various known concentrations of bovine serum albumin (BSA) as standards. The degree of BoNT/G activation averaged 76.7 ± 4.7% and was taken into account in toxicity calculations. GST−Syt fusion proteins were obtained from *E. coli* BL21 and purified employing glutathione-Sepharose beads (Macherey-Nagel GmbH & Co. KG, Düren, Germany). Fractions containing the desired proteins were pooled and dialyzed against Tris/NaCl/Triton buffer [20 mM Tris-HCl, 150 mM NaCl, and 0.5% Triton X-100 (pH 7.2)].

Ganglioside Binding Assay. Purified bovine brain gangliosides [GT1b, GD1b, GD1a, GM1a, and GM3 (Matreya, Pleasant Gap, PA)] were dissolved in DMSO and diluted in methanol to reach a final concentration of 27.2 μM; 100 μL each (5 μg for GT1b) was applied to each well of 96-well PVC assay plates [catalog no. 2595, Corning (Corning, NY)]. After evaporation of the solvent at 21 °C, the wells were washed with 200 μL of a PBS/0.1% (w/v) BSA mixture. Nonspecific binding sites were blocked by incubation for 1 h at 4 °C in 200 μL of a PBS/2% (w/v) BSA mixture. Binding assays were performed in 100 μL of a PBS/0.1% (w/v) BSA mixture per well for 3 h at 4 °C containing H_CG at the indicated concentrations (serial 3-fold dilution ranging from 5.4 μM to 0.09 nM). Following incubation, wells were washed twice with a PBS/0.1% (w/v) BSA mixture and then incubated with anti-FLAG monoclonal antibody M2 (1:4000, Sigma-Aldrich) for 1.5 h at 4 °C. After another washing step, the polyclonal rabbit anti-mouse antibody coupled with HRP (1:16000, IBA) was added for 1 h at 4 °C. Finally, after three washing steps with a PBS/0.1% (w/v) BSA mixture, bound H_CG was detected using Ultra TMB (100 μL/well, Thermo) as the substrate for HRP. The reaction was terminated after the mixture had been incubated for 40 min at 21 °C by the addition of 100 μL of 0.2 M H_2SO_4, and the absorbance at 450 nm was determined using a SpectraCount plate reader (Packard).

Data Analysis. Statistical analysis was performed using Prism (version 4.03, GraphPad). The EC_{50} values (nanomolar) of the ganglioside binding curves were determined by fitting the data to the sigmoidal dose−response equation employing the constraints BOTTOM = 0, TOP = shared, and HILLSLOPE = 1. Comparisons of means were performed using the two-tailed unpaired *t* test.

GST Pull-Down Assays. GST fusion proteins (0.15 nmol each) immobilized to 10 μL of glutathione-Sepharose beads at 4 °C were incubated with 0.1 nmol of wild-type or mutated H_C

dx.doi.org/10.1021/bi4003502 | *Biochemistry* 2013, 52, 3930−3938

fragment in a total volume of 150 μL of 20 mM Tris buffer (pH 7.2) supplemented with 0.5% Triton X-100 and 150 mM NaCl for 2 h at 4 °C. Beads were collected by centrifugation and washed three times each with 200 bed volumes of the same buffer. Washed pellet fractions were boiled in SDS sample buffer and analyzed by SDS−PAGE. Protein was detected by Coomassie Blue staining and quantified by using an LAS-3000 imaging system.

Mouse Phrenic Nerve (MPN) Toxicity Assay. The MPN toxicity assay was set up as described previously.[29,30] Electrical stimulation of the phrenic nerve was continuously performed at a frequency of 1 Hz. Isometric contractions were transformed via a force transducer and recorded with the VitroDat Online software (FMI GmbH). The time required to decrease the amplitude to 50% of the starting value (paralytic half-time) was measured. Concentration−response curves were recorded in triplicate for recombinant wild-type single-chain BoNT/B applying final concentrations of 0.1, 0.3, 1, and 3.2 nM and recombinant wild-type BoNT/G-Thro applied at final concentrations of 0.6, 2.0, 6.0, and 20.0 nM. The power functions $y = 54.368x^{-0.2947}$ ($R^2 = 0.9876$) and $y = 97.123x^{-0.2709}$ ($R^2 = 0.9967$) were fit to the data obtained for scBoNT/B and BoNT/G-Thro, respectively. The resulting paralytic half-times of scBoNT/B or BoNT/G-Thro mutants were converted to the corresponding concentrations of wild-type BoNTs using the equations mentioned above, and the toxicities were finally expressed as the percentage of the respective wild-type BoNT.

Molecular Dynamics Simulations. Molecular dynamics simulations were conducted using AMBER10 (http://ambermd.org/). All calculations used explicit solvent, and the protein was surrounded by an octahedral periodic box of TIP3P water molecules with a minimal distance of 10 Å from the solute before equilibration using a standard multistate protocol.[31] The PDB coordinates of H_CB−Syt-II (2NM1) and H_CG (2VXR) were used to obtain H_CG−Syt-I and H_CG−Syt-II models via SWISS-MODEL.[32] The unrestrained model complexes were simulated in explicit water solvent for 30 and 40 ns, respectively, at 310 K. The residue specific structure root-mean-square deviation (rmsd) was calculated using the PTRAJ module available within AMBER. Secondary structure analysis was performed using the Dictionary of Secondary Structure of Protein.[33]

RESULTS AND DISCUSSION

BoNT/G Preferentially Binds GT1b and GD1a. Prior studies showed that BoNT/A, -B, and -F bind gangliosides GT1b and GD1a with the highest affinity,[19−21] whereas BoNT/C, -DC, and -D preferentially interact with GD1b, GM1a, and GD2, respectively.[34,35] Structural alignments demonstrate that H_CG largely shares the conserved ganglioside binding pocket with the H_C fragment of BoNT/A, -B, -E, and -F and TeNT.[27,36] To functionally characterize the BoNT/G ganglioside binding pocket, we studied binding of various gangliosides using the microtiter well assay. At physiological salt concentrations, H_CG showed the highest affinity for GT1b (EC_{50} = 1.9 nM) and GD1a (EC_{50} = 2.5 nM). Considerable binding was also measured for GD1b (EC_{50} = 13.0 nM). GM3 exhibited weak binding (EC_{50} = 509 nM) and GM1a very weak binding (Figure 2). The determined order of affinity (GT1b > GD1a > GD1b) parallels that of the structurally related H_C fragments of BoNT/A, -B, and -F. Furthermore, these data show that BoNT/G requires the presence of the terminal sialic acid for optimal interaction as has been found for BoNT/A, -B, -E, and -F[19,22,37−39] and thus classifies BoNT/G into a joint group together with BoNT/A, -B, -E, and -F also in a functional respect. However, the mode of interaction with individual sugar units may vary to a certain extent within this group of BoNTs. First, the neurotoxicity in mice that lack GT1b and GD1b synthesis (GD3 synthetase deficient) is reduced to different degrees.[5] Second, replacement of the ganglioside binding motif residue histidine in H_CF with lysine, the homologous residue of BoNT/E-H_C, conferred binding to GM1a, although wild-type BoNT/E-H_C does not exhibit significant binding to GM1a.[37] It is likely that replacement of the H_CG structural homologue G1249 with lysine or histidine will increase its affinity for GM1a because mutation of the homologous histidine to alanine drastically reduced the affinity of BoNT/A and -B for gangliosides.

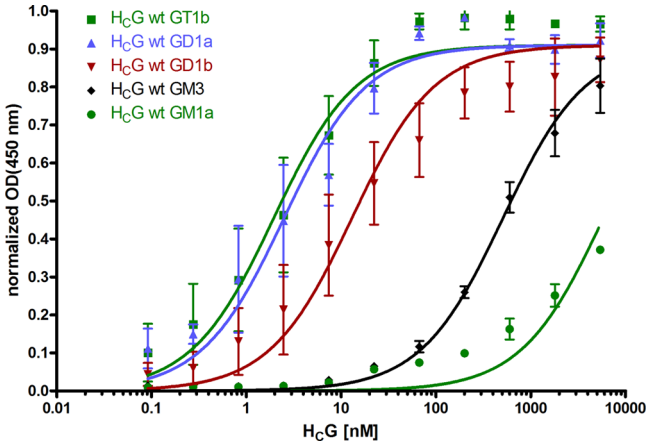

Figure 2. Analysis of binding of H_CG to various gangliosides. Binding of recombinant H_CG to immobilized gangliosides was examined at various H_C concentrations. EC_{50} values were determined by fitting the data to a sigmoidal dose−response curve model to be 1.944 nM for GT1b (95% confidence interval, 1.503−2.514 nM), 2.497 nM for GD1a (1.831−3.404 nM), 13.00 nM for GD1b (10.05−16.80 nM), 509.1 nM for GM3 (394.3−657.3 nM), and 5836 nM for GM1a (4047−8415 nM). Data represent means ± the standard deviation of four independent experiments performed in duplicate.

Three Amino Acids of Syt-II Differently Contribute to the Binding of BoNT/B and BoNT/G. To examine the role of the individual Syt-II amino acids in binding to BoNT/B and BoNT/G, we performed pull-down assays employing the mutated intravesicular domain of Syt-II fused to GST. Alanine was generally introduced except that E57 was substituted with lysine to evoke maximal differences in the effects on binding of BoNT/B-H_C (H_CB) and H_CG. N59, whose side chain points away from the H_CB−Syt-II interface,[25] was substituted with its homologue in Syt-I, a histidine. The results of these assays agree with data obtained previously for H_CB[25] and show that M46 of Syt-II is not and F47, F54, F55, and I58 are crucial for the interaction with both H_CB and H_CG (Figure 3). Thus, assuming that Syt-II also adopts a helical structure upon interaction with H_CG (discussed in a following section), we may conclude, though the Syt-II L50A mutation weakened the binding of H_CG somewhat more than the binding of H_CB, that the N-terminal [remote from the ganglioside binding pocket, W1268 (Figure 1A)] and central parts of the Syt-II helix are very similarly positioned in H_CB and H_CG. In contrast, positioning of the C-terminal part of the Syt-II helix (facing the ganglioside binding pocket) appears to differ between H_CB and H_CG. First, the Syt-II E57K mutation weakened binding of H_CB much more than binding of H_CG (Figure 3). This may be due to the induction of charge repulsion (Figure 1E) or clashes of K57 with H_CB K1192

dx.doi.org/10.1021/bi4003502 | Biochemistry 2013, 52, 3930−3938

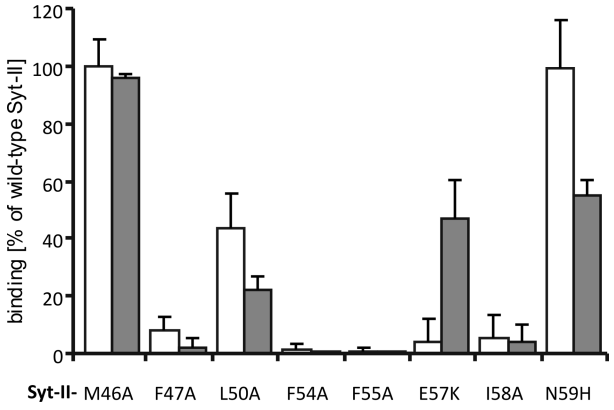

Figure 3. Analysis of binding of H_CB and H_CG to Syt-II mutants. GST-Syt-II(1−61) or its mutants (0.15 nmol each) bound to glutathione-Sepharose beads were incubated with H_CB or H_CG (0.1 nmol each) for 2 h. The amount of bound H_C fragment (molar ratio of GST-Syt to H_C) was determined following washing, SDS−PAGE, and Coomassie Blue staining by densitometry. Data represent the mean of three independent experiments ± the standard deviation shown as a percentage of the binding to wild-type GST-Syt-II(1−61). White and gray bars represent data for H_CB and H_CG, respectively.

and/or K1113. An explanation for the much weaker effect on H_CG binding might be the lack of charge repulsion and the larger distance of the homologous surface of H_CG formed by Q1200 and F1121. A bend in the C-terminal part of the Syt-II helix or breakup of its structure evoked by the interaction with H_CG is also conceivable (see below). Further evidence supporting this assumption is the observation that replacement of H_CG Q1200 with the homologous H_CB residue, lysine 1192, did not improve binding [no formation of a salt bridge with Syt-II E57 (Figures 1E and 4B)]. Second, mutant Syt-II N59H also led to different effects. Whereas binding of H_CB remained unaffected, the level of binding of H_CG was reduced to 54%. Though the amide side group of asparagine of Syt-II is facing away from the toxin−Syt-II interface, substitution with imidazole apparently interferes with the positioning of the Syt-II helix in H_CG but not in H_CB.

Mutations in the Central Part of the Syt-II Binding Site Exert Similar Drastic Effects on the Binding of BoNT/B and BoNT/G. Pull-down assays had previously shown that the affinities of H_CB and H_CG for Syt-I and Syt-II are quite dissimilar.[23] Because of the limited solubility of the recombinant H_CG in binding buffer, comparative numerical data for affinities could not be determined by employing methodologies like isothermal titration calorimetry. Nonetheless, H_CB bound with high affinity to the immobilized intravesicular domain of Syt-II (55.8 ± 11.6 mol % binding) but could not be precipitated by Syt-I. In contrast, H_CG bound both Syt-II and Syt-I, the latter with a somewhat higher affinity [22.0 ± 8.5 and 34.6 ± 10.3 mol % (p = 0.0034)]. To figure out the basis for these differences in protein receptor interactions, we conducted a systematic mutational analysis of all H_CB and H_CG residues supposed to be involved in Syt binding. First, we checked whether the residues forming the central part of the H_C−Syt interface fulfill the same tasks. These include conserved residues F1202, F1212, Y1189, A1204, and P1205 of H_CG (Figure 1A,B) and F1194, F1204, Y1181, A1196, and P1197 of H_CB (Figures 1B,E and 4A,B; BoNT/G amino acid numbering is generally shifted by eight positions compared to BoNT/B amino acid numbering within the Syt binding area). Equal substitutions were introduced. Each mutation in H_CG and H_CB nearly abolished binding, except that H_CB Y1181S showed merely residual binding, whereas the corresponding mutation in H_CG, Y1189S, decreased the binding affinity to approximately 42%. Thus, this region is crucial for binding of H_CB and H_CG, and positioning of the N-terminal part of the Syt-II helix in the conserved area appears to be virtually the same.

Replacement of BoNT/G Y1186 and L1191 with the Homologous BoNT/B Residues Causes a Substantial Increase in Syt-II Affinity. The amino acids surrounding the conserved central part of the binding site are not conserved. Therefore, residues of H_CG and H_CB were equally mutated, and most of them in addition reciprocally exchanged between H_CG and H_CB. Nonreciprocal exchanges in H_CG and H_CB had largely similar effects on Syt-II affinity. Mutations S1125D and M1126D in H_CG and their counterparts in H_CB (P1117D and V1118D) drastically reduced the level of binding. This result shows that amino acids exhibiting a negative charge in their side chain cannot be accommodated and underscores the necessity of hydrophobic or short side chains in this region. Also, the F1121M mutation in H_CG decreased the level of binding to a degree similar to that caused by the K1113M mutation in H_CB. Mutation of H_CG Q1200 to methionine or tyrosine did not affect the affinity of H_CG. The same mutations of its counterpart in H_CB, K1192, evoked a significant reduction in the level of binding (Figures 1A,C and 4A,B), whereas replacement with glutamic acid exerted a strong negative effect on H_CB but not on H_CG binding. This is likely due to charge repulsion by Syt-II E57 and agrees with binding data for mutant Syt-II E57K (Figure 3). H_CG N1207Y showed wild-type-like and H_CG T1199L as well as its homologue in H_CB (E1191L) moderately weakened binding, whereas H_CB S1199Y exhibited a 1.4-fold increased affinity (Figure 4A,B). Of the seven reciprocal mutations in the nonconserved surrounding area, all H_CB mutants exhibited 30−85% residual binding activity. In contrast, two of the seven BoNT/B counterparts assembled in H_CG almost abolished binding affinity for Syt-II (H_CG M1126V and H_CG A1124S). Whereas H_CB V1118M and H_CB S1116A still exhibit 30 and 75% residual binding, respectively, the more bulky side chain of valine and serine cannot be accommodated in the H_CG−Syt-II interface. The three mutations F1121K, S1125P, and Q1200K in H_CG led to a diminution of 20−40% in the level of binding similar to those of their counterparts in H_CB (K1113F, P1117S, and K1192Q). Apparently, introduction of a positive charge at position 1121 or 1200 of H_CG does not result in the formation of a salt bridge with Syt-II E57. As introduction of lysine even interferes with binding, one has to conclude that the side chains of these residues are located in the proximity of Syt, but in an unfavorable position for a positive contribution to binding. Strikingly different results were seen after introduction of BoNT/B-like side chains at positions 1186 and 1191 of H_CG, yielding H_CG Y1186W and H_CG L1191Y, respectively. The mutations increased the level of binding ∼2-fold (37.5 ± 11.7 mol % binding) and ∼3-fold (51.9 ± 16.6 mol % binding), respectively (Figures 1D and 4A,B). Hence, the affinity of H_CG L1191Y reached 93% of the level of H_CB binding. These data can be explained only if the interacting Syt segment also adopts an α-helical conformation upon contact with H_CG as has been demonstrated for H_CB[24,25] and occupies an overall similar position.

To confirm these data, we analyzed the effect of various mutations also in a physiological test system, the MPN assay, employing mutated full-length BoNTs. Data demonstrating the crucial importance of BoNT amino acids of the conserved central

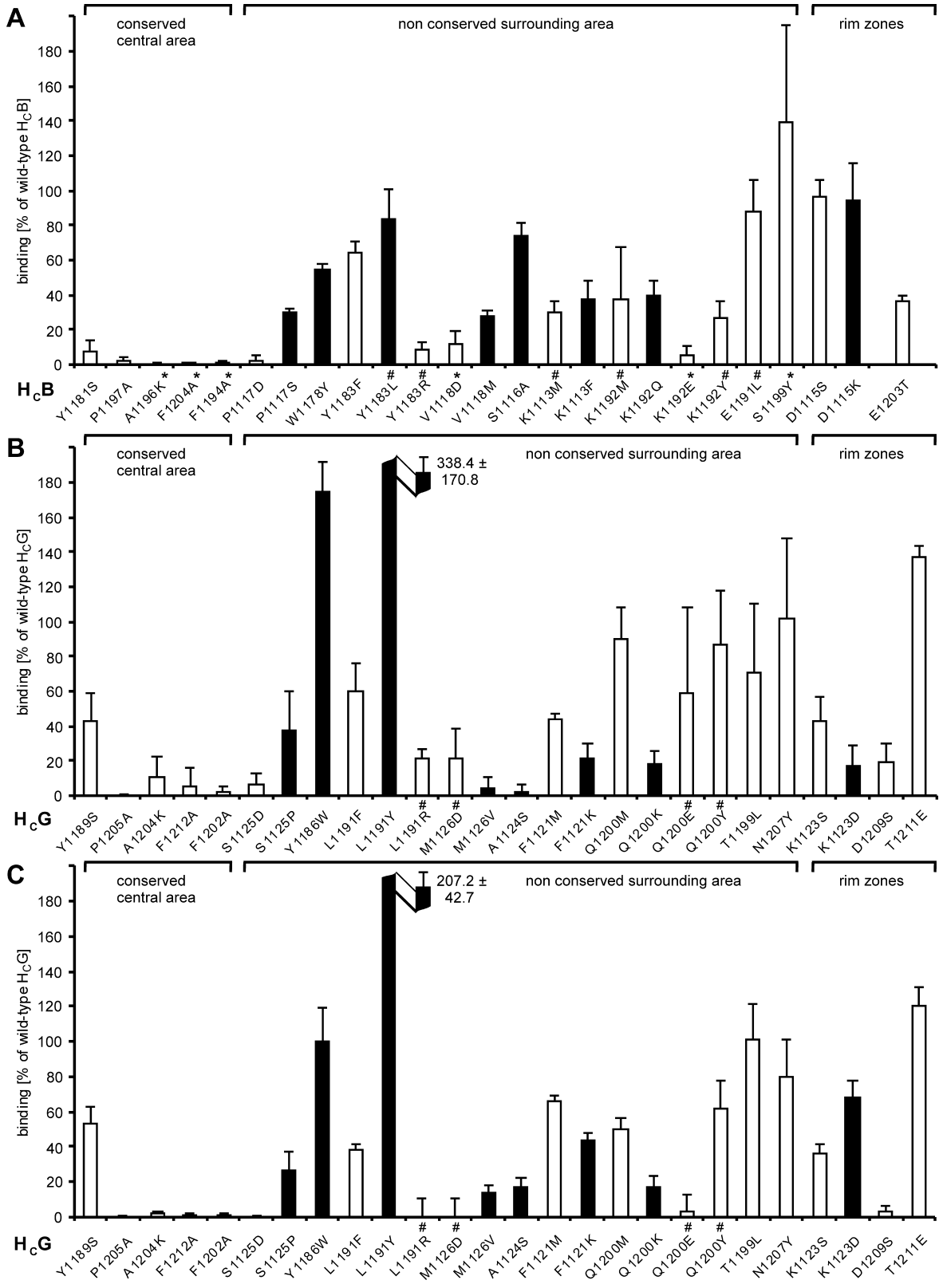

Figure 4. Analysis of binding of H_CB and H_CG mutants to Syt-I(1−53) and Syt-II(1−61). Wild-type or mutated H_CB (A) or H_CG (B and C) (0.1 nmol each) was added for 2 h to 0.15 nmol of either GST-Syt-II(1−61) (A and B) or GST-Syt-I(1−53) (C) immobilized to glutathione-Sepharose beads. The amount of bound H_C fragment (molar ratio of GST-Syt to H_C) was determined following washing, SDS−PAGE, and Coomassie Blue staining by densitometry. Data represent the mean of three to seven independent experiments ± the standard deviation shown as a percentage of wild-type binding. Asterisks[25] and number signs[23] denote previously published data. Black bars indicate reciprocal exchanges between H_CB and H_CG.

part of the Syt binding site have been published.[25] Here we focus our analysis on reciprocal mutations in the nonconserved surrounding area of BoNT/G. The mutations that impaired binding also caused a reduction in neurotoxicity (Figure 5);

dx.doi.org/10.1021/bi4003502 | *Biochemistry* 2013, 52, 3930−3938

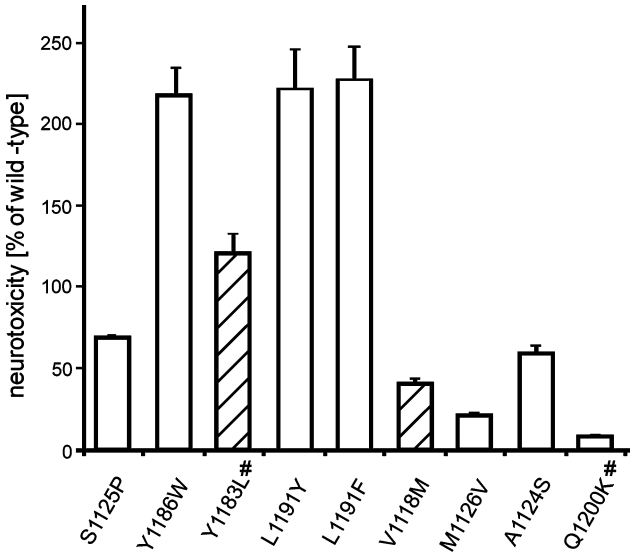

Figure 5. Toxicity of mutated scBoNT/B (hatched columns) and BoNT/G-Thro (white columns) in mouse phrenic nerve hemidiaphragm preparations. The mutants (except BoNT/G L1191F) each exhibit an amino acid reciprocally exchanged between BoNT/B and -G. Power functions were fit to dose−response curves of wild-type scBoNT/B and wild-type BoNT/G-Thro. Measured paralytic half-times of scBoNT/B or BoNT/G-Thro mutants were converted to the corresponding concentrations of wild-type BoNTs using the respective power function. The toxicities were finally expressed relative to the respective wild-type BoNT. Data represent mean values ± the standard deviation of at least three experiments. Number signs denote previously published data.[23]

however, the effects of the A1124S and S1125P mutations were significantly weaker than those on binding. Importantly, in the MPN assay, both BoNT/G mutations, Y1186W and L1191Y, which improved binding to Syt-II, also increased the neurotoxicity at the equivalent factor of ∼2.2. Hence, we may conclude that in addition to amino acids of the conserved part of the receptor−toxin interface only Y1186 and L1191 are located in exactly equivalent positions. Unlike the binding assay, L1191F improved neurotoxicity like L1191Y (Figure 4B). However, none of the three mutations in BoNT/G increased the biological activity to a value that compares to the activity of BoNT/B, because receptor binding is only one of several parameters that account for the toxicity.

Together, these results show that the majority of residues of the surrounding area contribute less to the overall affinity of H_CB and H_CG as their mutation caused less pronounced effects. Second, they suggest that the overall orientation of the Syt-II helix is the same in H_CG and H_CB, as mutation of equivalent residues of the binding area largely affects binding similarly. Being in line with this interpretation, two reciprocal mutations could evoke a drastic improvement in the binding affinity of H_CG. This together with the finding that vice versa none of the reciprocal mutations increased the affinity of H_CB underscores the better adaption of BoNT/B to Syt-II compared with BoNT/G and confirms the known higher affinity of H_CB versus that of H_CG. Evidence of subtle differences in the receptor helix positioning that should be based on differences in the surface configurations is provided by the function of the remaining amino acids present in the surrounding area and at rim positions. At rim positions, mutation of H_CB D1115 did not affect binding,

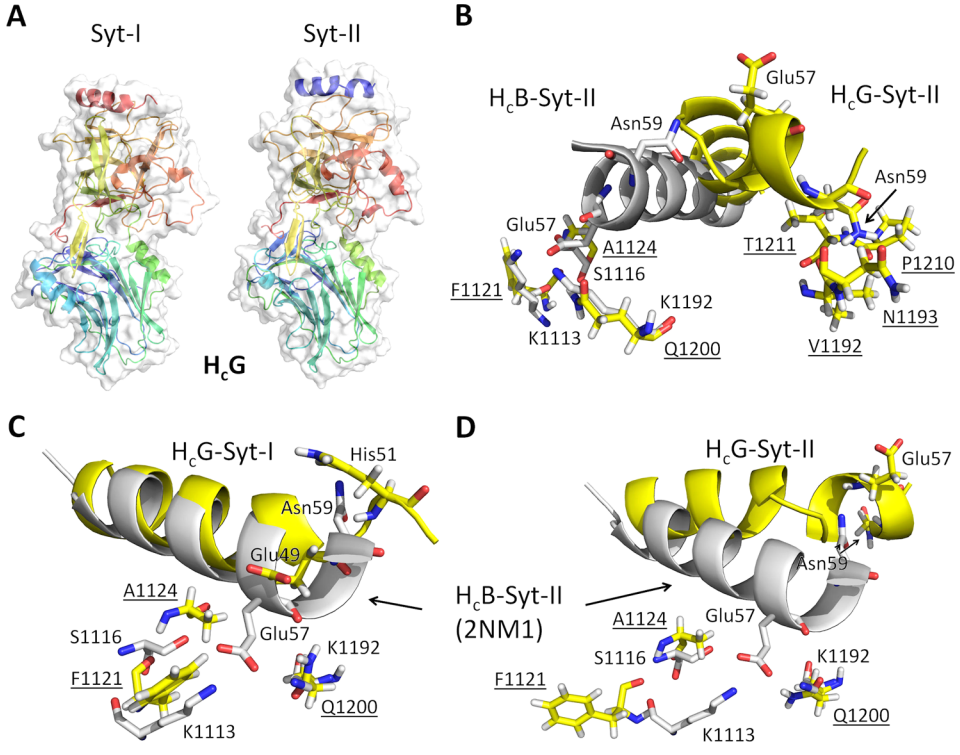

Figure 6. Molecular modeling studies of H_CG−Syt-I and H_CG−Syt-II complexes. (A) H_CG−Syt-I(36−52) and H_CG−Syt-II(44−60) final trajectories after 30 and 40 ns, respectively, unrestrained and in explicit water solvent. Both models are cartoons (rainbow colors, C-terminus colored red) showing the van der Waals surface (white) with 20% transparency. The orientation has been chosen to show Syts on top, Syt-I colored red, and Syt-II colored blue. (B−D) Close-ups of Syt bound to H_CG (yellow) and overlaid with H_CB−Syt-II (gray, 2NM1). Important residues are highlighted as sticks. Labeling: one-letter code for H_CB, one-letter code and underscore for H_CG, and three-letter code for Syt-I and Syt-II.

dx.doi.org/10.1021/bi4003502 | *Biochemistry* 2013, 52, 3930−3938

whereas the equivalent position in H_CG, K1123, appears to be involved in binding of Syt-II (Figure 4). Conversely, mutation of H_CB E1203, which is located on the opposite side of the binding area, negatively affected binding, as opposed to the likely equivalent of H_CG (T1211). Unlike in H_CB, in H_CG an additional residue, D1209, located adjacent to T1211, contributes to Syt binding at this rim position.

The Syt-I and Syt-II N-Terminal Domains Similarly Attach to BoNT/G-H_C. BoNT/G interacts more strongly with Syt-I than with Syt-II (see above and ref 23). To determine the molecular basis for this disparity, the effect of the H_CG mutations on binding was also assessed in pull-down experiments using the intravesicular domain of Syt-I. The extent of the effect was comparable for most mutations. However, binding to Syt-I was more unfavorably affected by mutations at positions Y1186, L1191, and Q1200 compared to that of Syt-II, whereas a greater reduction in the level of binding to Syt-II versus Syt-I was seen with H_CG A1124S and H_CG K1123D mutations and mutations of F1121 (Figure 4B,C).

To interpret these findings, it is important to know that the transmembrane-juxtaposed region of the intraluminal Syt domain mediates the interaction with BoNT/B and BoNT/G[14,18] and that three of the interacting amino acids differ between Syt isoforms I and II, namely, A38 versus M46, M47 versus F55, and L50 versus I58 (Figure 1E). As M46 marginally contributes to BoNT/B and BoNT/G binding[25] (Figure 3), substitution of only the two remaining positions in Syt-I with the corresponding Syt-II side chains converted Syt-I into a Syt-II-like high-affinity receptor for BoNT/B.[25] In analogy to the H_CB–Syt-II interface, Y1186 of H_CG is supposed to interact with Syt-II M46 and H_CG L1191 with F55 and I58. Interestingly, these are the three positions that differ in Syt-I. Tryptophan instead of tyrosine at position 1186 improved the interaction with Syt-II but did not increase the affinity for Syt-I. Similarly, tyrosine instead of leucine at position 1191 increased the level of binding of H_CG to Syt-II much more than the level of binding to Syt-I. On the basis of the smaller increase in affinity for Syt-I, we conclude that the side chains of Y1186 and L1191 of wild-type H_CG are inherently better adapted to A38 and M47/L50 of Syt-I, respectively, as compared to M46, F55, and I58 of Syt-II and may thus mediate the higher affinity of H_CG for Syt-I compared to that for Syt-II. An interpretation of the stronger effect of Q1200 mutations on Syt-I is challenging, as Q1200 is located in the sphere of E57 that is conserved in Syt-I (E49). An explanation might be a slightly different positioning of Syt-I at one rim zone of the toxin–receptor interface. This might also explain the stronger effects of the K1123D, A1124S, F1121M, and F1121K mutations on Syt-II binding versus Syt-I (Figure 4B,C), because they all are located in the proximity of E57 and E49, respectively.

Molecular Modeling Identifies Different Lengths and Bends in Syt Helices Adopted upon Contact with H_CB or H_CG. To confirm the conclusions drawn from the binding data, possible modes of binding of Syt-I (E36–K52) and Syt-II (E44–K60) to BoNT/G were explored. Both protein receptors were modeled into the binding site of H_CG using the PDB coordinates of H_CB–Syt-II (2NM1[25]) and H_CG (2VXR[27]). Note that the sequences of H_CB and H_CG are 43% identical and that H_CB and H_CG show great similarities in their receptor binding specificities. After initial equilibration of the new H_CG–Syt models, a trajectory of 40 ns has been simulated for each complex unrestrained and in explicit solvent. Figure 6 shows the coordinates of the final trajectory of H_CG–Syt-I and H_CG–Syt-II (A) and a close-up of Syt highlighting important residues in H_CG (B–D, yellow) and overlaid with H_CB–Syt-II (B–D, gray). Importantly, in both cases, the Syt molecule loses helical character at the C-terminus and bends toward the V1192–Q1198 loop, more severely for Syt-II than for Syt-I (Figure 6). In particular, while Syt-II E57 establishes contacts with K1113, S1116, and K1192 in H_CB, the corresponding contacts are lost in the final trajectory of H_CG–Syt-II (Figure 6B). However, new interactions are possibly formed between Syt-II N59 and H_CG (P1210, T1211, V1192, and N1193), which are absent in H_CB–Syt-II (Figure 6B). Except for an unsolved function of H_CG K1123 in binding, the modeling data are consistent with results obtained by pull-down and *ex vivo* toxicity assays (Figures 3 and 4) and underline the power of combining experimental and computational methods to study protein–protein interactions. Furthermore, both Syt conformations in H_CG are adopted within the first couple of nanoseconds of the simulation and proved to be stable during the remainder of the experiment, indicating the capture of one possible low-energy conformer sampled during H_CG–Syt recognition. Together, a vast amount of *in vitro* and *ex vivo* results combined with molecular modeling studies conducted on the basis of H_CB–Syt-II (2NM1) and H_CG (2VXR) X-ray data support similar helical modes of binding of Syt to the receptor binding H_C fragments of BoNT/B and BoNT/G. A significant part of the difference in affinity between H_CG and Syt-I and Syt-II compared to that between H_CB and Syt-II is most likely due to weaker interactions of the C-terminal part of the Syt helix with H_CG, which might lead to partially unraveling and/or bending of the helix. Future X-ray crystallography and NMR studies will probe in atomistic detail the compiled models of H_CG–Syt interaction.

AUTHOR INFORMATION

Corresponding Author

*Phone: +49 511 532 2859. E-mail: binz.thomas@mh-hannover.de.

Funding

This work was supported in part by grants from Deutsche Forschungsgemeinschaft (Project Bi 660/2-3 to T.B. and Exzellenzinitiative GSC108 to G.W.) and from Robert Koch-Institut (1362/I-979 to A.R.).

Notes

The authors declare no competing financial interest.

ACKNOWLEDGMENTS

We thank T. Henke and N. Krez for excellent technical assistance.

ABBREVIATIONS

BoNT, botulinum neurotoxin; BoNT/X, botulinum neurotoxin serotype X; H_C, C-terminal half of botulinum neurotoxin heavy chain; H_CX, H_C of serotype X; MPN, mouse phrenic nerve; PDB, Protein Data Bank; SNAP-25, synaptosomal-associated protein of 25 kDa; Syt, synaptotagmin; VAMP, vesicle-associated membrane protein.

REFERENCES

(1) Hill, K. K., and Smith, T. J. (2013) Genetic Diversity Within *Clostridium botulinum* Serotypes, Botulinum Neurotoxin Gene Clusters and Toxin Subtypes. *Curr. Top. Microbiol. Immunol. 364*, 1–20.

(2) Swaminathan, S. (2011) Molecular structures and functional relationships in clostridial neurotoxins. *FEBS J. 278*, 4467–4485.

(3) Montal, M. (2010) Botulinum neurotoxin: A marvel of protein design. *Annu. Rev. Biochem. 79*, 591−617.
(4) Binz, T. (2013) Clostridial Neurotoxin Light Chains: Devices for SNARE Cleavage Mediated Blockade of Neurotransmission. *Curr. Top. Microbiol. Immunol. 364*, 139−157.
(5) Rummel, A. (2013) Double Receptor Anchorage of Botulinum Neurotoxins Accounts for their Exquisite Neurospecificity. *Curr. Top. Microbiol. Immunol. 364*, 61−90.
(6) Karalewitz, A. P., Fu, Z., Baldwin, M. R., Kim, J. J., and Barbieri, J. T. (2012) Botulinum neurotoxin serotype C associates with dual ganglioside receptors to facilitate cell entry. *J. Biol. Chem. 287*, 40806−40816.
(7) Strotmeier, J., Gu, S., Jutzi, S., Mahrhold, S., Zhou, J., Pich, A., Eichner, T., Bigalke, H., Rummel, A., Jin, R., and Binz, T. (2011) The biological activity of botulinum neurotoxin type C is dependent upon novel types of ganglioside binding sites. *Mol. Microbiol. 81*, 143−156.
(8) Binz, T., and Rummel, A. (2009) Cell entry strategy of clostridial neurotoxins. *J. Neurochem. 109*, 1584−1595.
(9) Dong, M., Liu, H., Tepp, W. H., Johnson, E. A., Janz, R., and Chapman, E. R. (2008) Glycosylated SV2A and SV2B mediate the entry of botulinum neurotoxin E into neurons. *Mol. Biol. Cell 19*, 5226−5237.
(10) Dong, M., Yeh, F., Tepp, W. H., Dean, C., Johnson, E. A., Janz, R., and Chapman, E. R. (2006) SV2 Is the Protein Receptor for Botulinum Neurotoxin A. *Science 312*, 592−596.
(11) Mahrhold, S., Rummel, A., Bigalke, H., Davletov, B., and Binz, T. (2006) The synaptic vesicle protein 2C mediates the uptake of botulinum neurotoxin A into phrenic nerves. *FEBS Lett. 580*, 2011−2014.
(12) Peng, L., Tepp, W. H., Johnson, E. A., and Dong, M. (2011) Botulinum neurotoxin D uses synaptic vesicle protein SV2 and gangliosides as receptors. *PLoS Pathog. 7*, e1002008.
(13) Rummel, A., Hafner, K., Mahrhold, S., Darashchonak, N., Holt, M., Jahn, R., Beermann, S., Karnath, T., Bigalke, H., and Binz, T. (2009) Botulinum neurotoxins C, E and F bind gangliosides via a conserved binding site prior to stimulation-dependent uptake with botulinum neurotoxin F utilising the three isoforms of SV2 as second receptor. *J. Neurochem. 110*, 1942−1954.
(14) Dong, M., Richards, D. A., Goodnough, M. C., Tepp, W. H., Johnson, E. A., and Chapman, E. R. (2003) Synaptotagmins I and II mediate entry of botulinum neurotoxin B into cells. *J. Cell Biol. 162*, 1293−1303.
(15) Dong, M., Tepp, W. H., Liu, H., Johnson, E. A., and Chapman, E. R. (2007) Mechanism of botulinum neurotoxin B and G entry into hippocampal neurons. *J. Cell Biol. 179*, 1511−1522.
(16) Nishiki, T., Kamata, Y., Nemoto, Y., Omori, A., Ito, T., Takahashi, M., and Kozaki, S. (1994) Identification of protein receptor for *Clostridium botulinum* type B neurotoxin in rat brain synaptosomes. *J. Biol. Chem. 269*, 10498−10503.
(17) Peng, L., Berntsson, R. P., Tepp, W. H., Pitkin, R. M., Johnson, E. A., Stenmark, P., and Dong, M. (2012) Botulinum neurotoxin D-C uses synaptotagmin I and II as receptors, and human synaptotagmin II is not an effective receptor for type B, D-C and G toxins. *J. Cell Sci. 125*, 3233−3242.
(18) Rummel, A., Karnath, T., Henke, T., Bigalke, H., and Binz, T. (2004) Synaptotagmins I and II act as nerve cell receptors for botulinum neurotoxin G. *J. Biol. Chem. 279*, 30865−30870.
(19) Fu, Z., Chen, C., Barbieri, J. T., Kim, J. J., and Baldwin, M. R. (2009) Glycosylated SV2 and gangliosides as dual receptors for botulinum neurotoxin serotype F. *Biochemistry 48*, 5631−5641.
(20) Kozaki, S., Ogasawara, J., Shimote, Y., Kamata, Y., and Sakaguchi, G. (1987) Antigenic structure of *Clostridium botulinum* type B neurotoxin and its interaction with gangliosides, cerebroside, and free fatty acids. *Infect. Immun. 55*, 3051−3056.
(21) Simpson, L. L., and Rapport, M. M. (1971) The binding of botulinum toxin to membrane lipids: Sphingolipids, steroids and fatty acids. *J. Neurochem. 18*, 1751−1759.
(22) Stenmark, P., Dupuy, J., Imamura, A., Kiso, M., and Stevens, R. C. (2008) Crystal structure of botulinum neurotoxin type A in complex with the cell surface co-receptor GT1b-insight into the toxin-neuron interaction. *PLoS Pathog. 4*, e1000129.
(23) Rummel, A., Eichner, T., Weil, T., Karnath, T., Gutcaits, A., Mahrhold, S., Sandhoff, K., Proia, R. L., Acharya, K. R., Bigalke, H., and Binz, T. (2007) Identification of the protein receptor binding site of botulinum neurotoxins B and G proves the double-receptor concept. *Proc. Natl. Acad. Sci. U.S.A. 104*, 359−364.
(24) Chai, Q., Arndt, J. W., Dong, M., Tepp, W. H., Johnson, E. A., Chapman, E. R., and Stevens, R. C. (2006) Structural basis of cell surface receptor recognition by botulinum neurotoxin B. *Nature 444*, 1096−1100.
(25) Jin, R., Rummel, A., Binz, T., and Brunger, A. T. (2006) Botulinum neurotoxin B recognizes its protein receptor with high affinity and specificity. *Nature 444*, 1092−1095.
(26) Sonnabend, O., Sonnabend, W., Heinzle, R., Sigrist, T., Dirnhofer, R., and Krech, U. (1981) Isolation of *Clostridium botulinum* type G and identification of type G botulinal toxin in humans: Report of five sudden unexpected deaths. *J. Infect. Dis. 143*, 22−27.
(27) Stenmark, P., Dong, M., Dupuy, J., Chapman, E. R., and Stevens, R. C. (2010) Crystal structure of the botulinum neurotoxin type G binding domain: Insight into cell surface binding. *J. Mol. Biol. 397*, 1287−1297.
(28) Rummel, A., Mahrhold, S., Bigalke, H., and Binz, T. (2004) The HCC-domain of botulinum neurotoxins A and B exhibits a singular ganglioside binding site displaying serotype specific carbohydrate interaction. *Mol. Microbiol. 51*, 631−643.
(29) Habermann, E., Dreyer, F., and Bigalke, H. (1980) Tetanus toxin blocks the neuromuscular transmission in vitro like botulinum A toxin. *Naunyn-Schmiedeberg's Arch. Pharmacol. 311*, 33−40.
(30) Wohlfarth, K., Goschel, H., Frevert, J., Dengler, R., and Bigalke, H. (1997) Botulinum A toxins: Units versus units. *Naunyn-Schmiedeberg's Arch. Pharmacol. 355*, 335−340.
(31) Shields, G. C., Laughton, C. A., and Orozco, M. (1997) Molecular dynamics simulations of the d(T·A·T) triple helix. *J. Am. Chem. Soc. 119*, 7463−7469.
(32) Arnold, K., Bordoli, L., Kopp, J., and Schwede, T. (2006) The SWISS-MODEL workspace: A web-based environment for protein structure homology modelling. *Bioinformatics 22*, 195−201.
(33) Kabsch, W., and Sander, C. (1983) Dictionary of protein secondary structure: Pattern recognition of hydrogen-bonded and geometrical features. *Biopolymers 22*, 2577−2637.
(34) Karalewitz, A. P., Kroken, A. R., Fu, Z., Baldwin, M. R., Kim, J. J., and Barbieri, J. T. (2010) Identification of a unique ganglioside binding loop within botulinum neurotoxins C and D-SA. *Biochemistry 49*, 8117−8126.
(35) Kroken, A. R., Karalewitz, A. P., Fu, Z., Kim, J. J., and Barbieri, J. T. (2011) Novel ganglioside-mediated entry of botulinum neurotoxin serotype D into neurons. *J. Biol. Chem. 286*, 26828−26837.
(36) Schmitt, J., Karalewitz, A., Benefield, D. A., Mushrush, D. J., Pruitt, R. N., Spiller, B. W., Barbieri, J. T., and Lacy, D. B. (2010) Structural analysis of botulinum neurotoxin type G receptor binding. *Biochemistry 49*, 5200−5205.
(37) Benson, M. A., Fu, Z., Kim, J. J., and Baldwin, M. R. (2011) Unique ganglioside recognition strategies for clostridial neurotoxins. *J. Biol. Chem. 286*, 34015−34022.
(38) Ochanda, J. O., Syuto, B., Ohishi, I., Naiki, M., and Kubo, S. (1986) Binding of *Clostridium botulinum* neurotoxin to gangliosides. *J. Biochem. 100*, 27−33.
(39) Ogasawara, J., Kamata, Y., Sakaguchi, G., and Kozaki, S. (1991) Properties of a protease-sensitive acceptor component in mouse brain synaptosomes for *Clostridium botulinum* type B neurotoxin. *FEMS Microbiol. Lett. 63*, 351−355.